PSU-IRL-SCI 376

THE PENNSYLVANIA STATE UNIVERSITY

IONOSPHERIC RESEARCH

Scientific Report 376(E)

INTEGRATED CIRCUIT ELECTROMETER AND SWEEP CIRCUITRY FOR AN ATMOSPHERIC PROBE

by

Larry Eugene Zimmerman

November 1, 1971

The research reported in this document has been sponsored by the National Aeronautics and Space Administration under Grant NGL-009-0015.

IONOSPHERE RESEARCH LABORATORY

University Park, Pennsylvania

PSU - IRL - SCI 376

Scientific Report 376(E)

"Integrated Circuit Electrometer and Sweep Circuitry For an Atmospheric Probe"

by

Larry Eugene Zimmerman

November 1, 1971

"The research reported in this document has been sponsored by the National Aeronautics and Space Administration under Grant NGL-009-0015."

Submitted by: Leslie C. Hale

Leslie C. Hale, Professor of Electrical Engineering, Project Supervisor

Approved by: John S. Nisbet

John S. Nisbet, Director
Ionosphere Research Laboratory

Ionosphere Research Laboratory

The Pennsylvania State University

University Park, Pennsylvania 16802

ACKNOWLEDGMENTS

The author wishes to express his thanks to Dr. Leslie C. Hale for his assistance and guidance in this investigation.

TABLE OF CONTENTS

LIST OF TABLES

LIST OF FIGURES

CHAPTER I

INTRODUCTION

1.1 Statement of the Problem

Atmospheric electrical structure measurements are performed by a variety of techniques, but one of the simplest involves the use of metallic probes. This technique involves the measurement of the current to a conducting surface which is charged to a known potential with respect to the ambient medium via a second electrode. Using a known relationship between the known potential, measured probe current, and the parameters of the ambient medium, one may deduce the values of these parameters (Willis, 1965). The mechanics by which such probes collect charged particles are in general quite complex, but reduce to simple, easily interpreted situations in some special cases, such as:

1. The ram positive ion current to a very rapidly moving probe (Hale, 1964; Hoffman, 1966; Pontano, 1967) in the "free molecular flow" case.
2. The simple mobility theory (Hoult, 1965; Sonin, 1967) governing the collection of charged particles by a moving probe in the continuum situation. An example of the implementation of such a probe is the "parachute-borne blunt probe" (Hale, Hoult, and Willis, 1966; Hale, Hoult, and Bake, 1968).

We are concerned here with the second case. A probe moving in a continuum has a tendency to measure conductivity to the exclusion of information about number density, which is frequently the quantity

desired. (It should be noted here that in many cases conductivity is really the more important quantity, particularly in the case of VLF and ELF radio wave propagation.) Conductivity is the product of number density times mobility, and hence information is required about charged particle mobility.

The "Gerdien condenser" can in theory provide information about conductivity and density. In practice it suffers from end effects and sensitivity to angle of attack and other flow variables. Various forms of "mobility spectrometers" (Hoult and Kuo, 1967) have been proposed, but are subject to various defects (Keller, 1968). However, it appears worthwhile to experimentally evaluate some schemes for the direct measurement of mobility. The "small signal" scheme of Hoult and Kuo (1967) was found to be lacking in resolution and sensitivity in practical upper atmospheric situations, and hence a "large signal" approach was proposed by Hale (1968). Basically this consists of measuring the response of a stationary probe to a step of voltage. Stationary probes may be balloon borne or may be fixed on the surface of a planet (under very low wind conditions). Hoult (1968) has suggested a "soda - straw honeycomb" probe geometry for ameliorating the deleterious effects of wind in the stationary case or probe motion. Such stationary probes must be at essentially zero potential prior to the application of a large voltage step, and the information on mobility is contained in the subsequent i(t) waveform. A variety of questions remain about such probes which require experimental observation for their resolution.

The instrumentation problems of geometry, a suitable sweep waveform, and a current measuring system to implement the type of measuring system described above were found to be non-trival. The electronics is required to be simple, light, and rugged with very low power consumption. The electrometer must be protected from large overloads and, particularly, must recover rapidly from large displacement current spikes due to the voltage step in order to accurately determine the subsequent i(t) waveform. The sweep waveform must have a fast rise time from zero volts. The amplitude must be several volts to reduce errors due to vehicle potential effects which shift the effective zero potential up and down the sweep waveform (Hale, 1967). Also, the sweep rate should be chosen to reduce displacement current effects to an acceptable level.

The above requirements lead to the sweep waveform shown in Figure 1 and the electrometer design to be discussed.

1.2 Small Current Measurement

In electrometer applications, the problem is normally to transduce a current in the range of 10^{-7} to 10^{-14} amperes into a voltage. To accomplish this low level measurement generally requires a high input impedance device. The two basic types of devices most suited are the capacitor modulated A. C. amplifier and the D. C. electrometer amplifier. The former classification consists of the vibrating reed capacitor modulator and the varactor bridge modulator. For probe applications, one may dismiss the vibrating reed capacitor modulator due to its large size, high power

requirements, complexity, and cost. Amplifiers with varactor bridge inputs can achieve input bias currents on the order of 10^{-14} amperes but have disadvantages of asymetrical input currents, limited bandwidth, and an internal oscillator which must be carefully shielded to minimize radiated noise. In addition, there is a dependency upon the bridge capacitors maintaining their capacitance within close tolerances so as not to introduce offset voltages. With respect to the D. C. electrometer amplifier, electrometer tubes and MOSFET's may be considered for the input stage. However, with the drift and microphonics associated with electrometer tubes, MOSFET's appear to be better suited. When provided with protection against static voltages discharging through the gate-oxide layer, MOSFET's are quite reliable in applications requiring low input current.

1.3 Sweep Waveform

The sweep waveform is shown in Figure 1. Through slight modifications of the sweep circuit, the waveform may be rectified positively or negatively. A triangular waveform is also generated by the sweep circuitry.

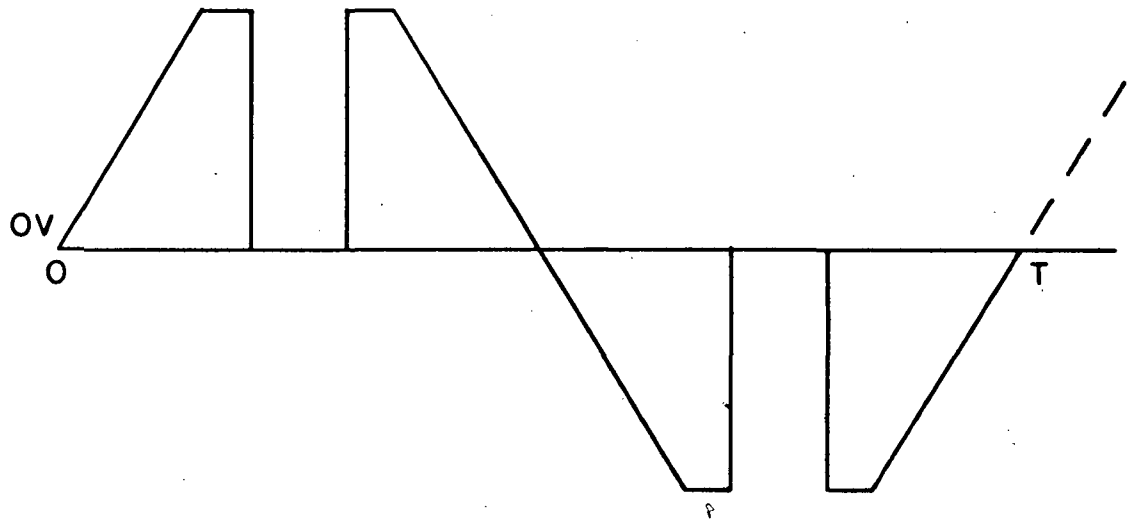

SWEEP WAVEFORM

FIGURE 1

CHAPTER II

ELECTROMETER APPLICATION OF AN INTEGRATED CIRCUIT OPERATIONAL AMPLIFIER

2, 1 Selection of a Suitable Operational Amplifier

The first and most important consideration must be the input bias current and its stability with temperature. The input bias current should be less than 10% of the smallest current anticipated to be measured and have stability over the temperature range of interest. Secondly, it should be determined if protection of the input device is required and if such protection will introduce leakage currents. In addition, the amplifier should have an offset null capability and a frequency response appropriate for the input signal.

2.2 Description of the ICH8500A Integrated Circuit Operational Amplifier

The ICH8500A is a hybrid integrated circuit operational amplifier by Intersil, Incorporated. Designed for ultra low input bias current applications, it contains two P-channel enhancement mode MOSFET's as the input device, a J-FET constant current source, and an integrated circuit amplifier on a chip. The schematic and connection diagrams are shown in Figure 2a and 2b. Electrical characteristics are listed in Table 1. The ultra low input bias current is achieved by eliminating practically all header leakage currents which, in MOS-input devices, account for the largest portion of the input bias current. Thus, with the case (pin 8) at the same potential as the input leads, any current flow between the case and the input pins is eliminated. In addition, any leakage

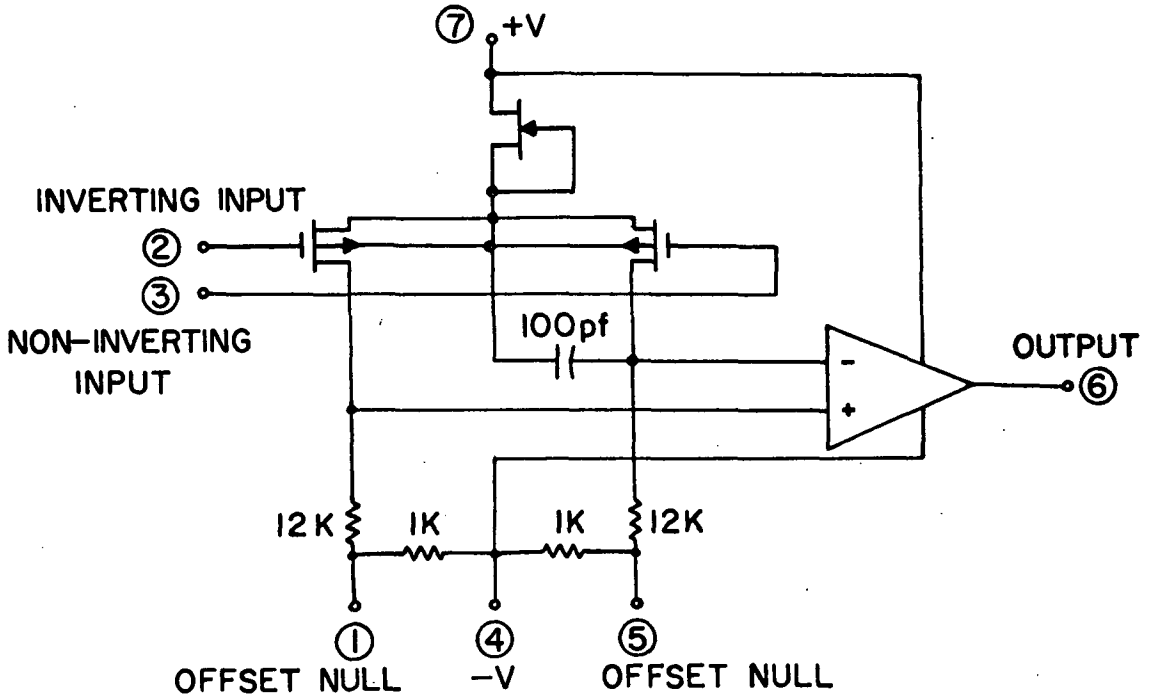

a. SCHEMATIC DIAGRAM

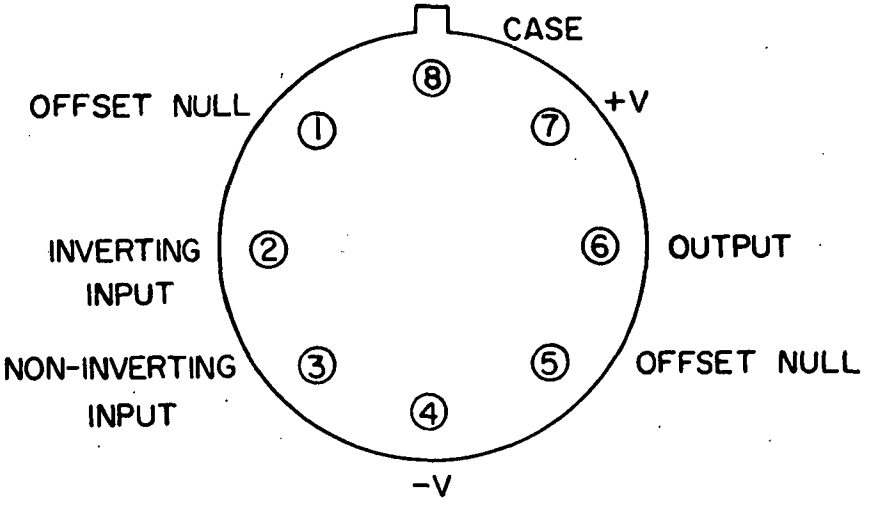

b. CONNECTION DIAGRAM (TOP VIEW)

THE ICH8500A INTEGRATED CIRCUIT

FIGURE 2

TABLE 1

ELECTRICAL CHARACTERISTICS OF THE ICH8500A INTEGRATED CIRCUIT

Maximum Ratings

Supply Voltage	± 18V
Internal Power Dissipation*	500 mW
Differential Voltage	± 100V
Storage Temperature	-65°C to +150°C
Operating Temperature	-25°C to +85°C
Lead Temperature (Soldering 60 sec)	300°C
Output Short Circuit Duration	Indefinite

Electrical Specifications

(T_A = 25°C unless otherwise stated, V_s = ± 15V)

Characteristic	Min	Typ	Max	Units	Test Conditions
Input Leakage Current (Inverting and Non-Inverting)			.01	pA	Case at Same Potential as Inputs
Input Offset Voltage		5	20	mV	
Offset Voltage Adjustment Range			±25	mV	2K Potentiometer
Change in Input Offset Voltage over Temperature			±5 ±5	mV mV	+25 to 75°C -25 to +25°C
Common Mode Rejection Ratio	60	75		dB	±5 volts Common Mode Voltage
Output Voltage Swing	±12	±14		V	$R_L \geq$ 10K
Common Mode Voltage Range	±10			V	

TABLE 1 (Continued)

Characteristic	Min	Typ	Max	Units	Test Conditions
Large Signal Voltage Gain	20,000	10^5			
Feedback Capacitance			.1	pF	Case Guarded
Long Term Input Offset Voltage Stability			±3	mV	At 25°C
Slew Rate		.5		v/μS	$R_L \geq$ 2K

* Rating applies for ambient temperatures to + 70°C.

currents that may have existed between any of the other pins and the inputs are now intercepted by the case since the case completely encircles every pin on the header.

CHAPTER III

ELECTROMETER DESIGN

3.1 Design Considerations

The basic circuits for response time analysis is shown in Figure 3. An amplifier of gain A is connected in the inverting mode with C_1 representing the sum of the input capacitance, and C_2 representing a lumped stray capacitance across the resistor R_F. For the purpose of circuit analysis, let Figure 3a be modified as shown in Figure 3b. The input current is

$$I_{in} = V_{in} p C_1 + [V_{in} - B\,Vo] \frac{1 + p\,C_2 R_F}{R_F} \tag{1}$$

where p is the differential operator. Rearranging,

$$I_{in} = - V_o \left[\frac{p C_1}{A} + \frac{1 + p\,C_2 R_F}{A R_F} + \frac{B(1 + pC_2 R_F)}{R_F} \right]. \tag{2}$$

If the circuit is excited by a current square wave, the output voltage is

$$V_o = - \frac{I_{in} R_F A}{1 + BA} \left[1 - \exp\left\{ \frac{-t}{R_F \left(\frac{C_1}{1 + BA} + C_2 \right)} \right\} \right]. \tag{3}$$

The time constant is then

$$T = R_F \left[\frac{C_1}{1 + BA} + C_2 \right] \tag{4}$$

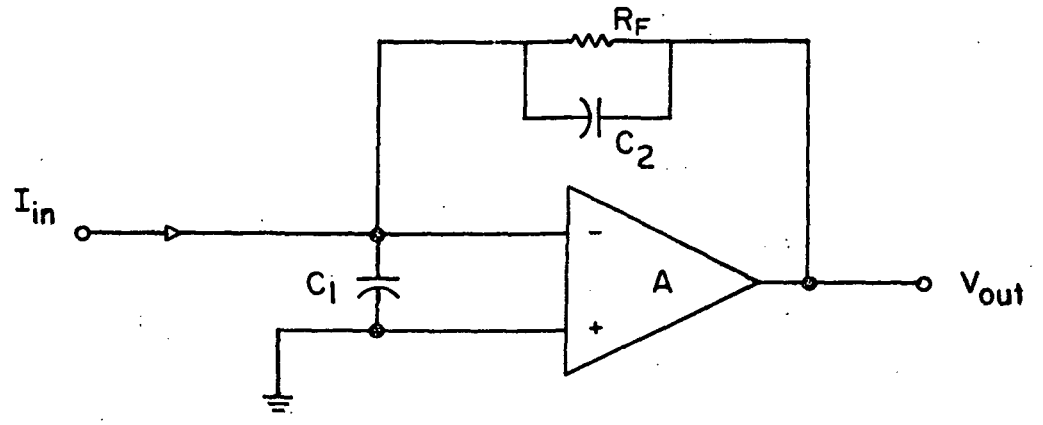

a. FEEDBACK ELECTROMETER

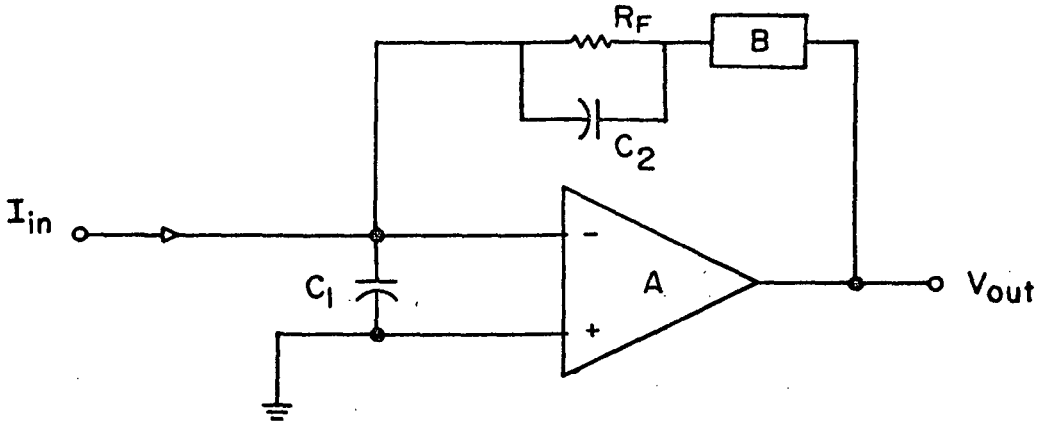

b. FEEDBACK ELECTROMETER WITH COMPENSATION NETWORK

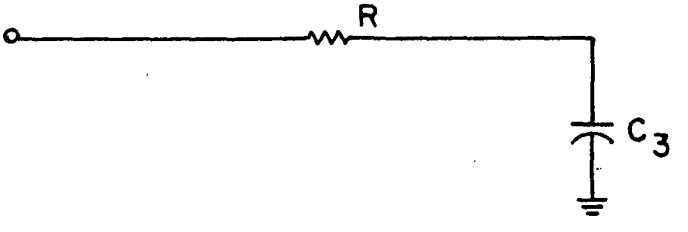

c. COMPENSATION NETWORK

NETWORKS FOR RESPONSE TIME ANALYSIS

FIGURE 3

where the time constant formed by the input capacitance, $R_F C_1$, is reduced by "1 + BA". However, $R_F C_2$, the time constant formed by the feedback resistor and its associated stray capacitance, is not affected. Thus, to improve the response time, $R_F C_2$ must be neutralized. To accomplish this, let the box labeled "B" in Figure 3b have the form of the network shown in Figure 3c. The transfer function of this network is

$$B = \frac{1}{1 + pC_3R} . \tag{5}$$

If this is then substituted for "B" in Equation (2) and if $C_3R = C_2R_F$, then the third term becomes $\frac{1}{R_F}$. Now the network response to a current step is

$$V_o = - \frac{I_{in} R_F A}{A + 1} \left[1 - \exp \left\{ \frac{-t}{R_F \frac{C_1 + C_2}{A + 1}} \right\} \right] \tag{6}$$

where the time constant is now,

$$T = \frac{R_F (C_1 + C_2)}{A + 1} . \tag{7}$$

The preceeding analysis has ignored the stray capacitance that is distributed along the feedback units. The performance then resembles that of a delay line making perfect compensation impossible. However, a significant improvement may be achieved through the analysis discussed.

A possible method of measuring an amplifier's response to a current step input is the "injection capacitor" method as described by Praglin and Nichols (1960). A triangle voltage waveform is applied to the amplifier through a small capacitance, C_4, thus generating a current square wave. The amplifier response including C_4 is,

$$V_o = -\frac{aR_F C_4 A}{1+A}\left[1 - \exp\left(\frac{-t}{R_F\left[\frac{C_4 + C_1}{1+A} + C_2\right]}\right)\right] \quad (8)$$

where a is the slope of the ramp input. The time constant is

$$T = R_F\left[\frac{C_4 + C_1}{1+A} + C_2\right]. \quad (9)$$

Thus if C_4 is much smaller than C_1, the error in rise time caused by the current injecting capacitor is negligible.

In working with picoamp signals, attention to leakage resistance is extremely important. For example, a leakage resistance of 10^{14} ohms from a 15 volt power supply to the input of the ICH8500A will cause a .15pA error current which is 15 times the input bias current of the amplifier. The insulation resistance of most commercial wire and printed circuit boards is less than 10^{14} ohms, particularly on a humid day. To eliminate leakage currents, the input leads may be completely surrounded by a potential near that of the input. Leakage currents will then be intercepted before reaching the electrometer input. Another method is to place the input on a material having a high resistivity such as teflon, Kel-F, polystyrene, or

sapphire. Still another method is to float the input lead and pot the electrometer in an insulating material such as paraffin.

Rigidity of construction is another important consideration. Motion of leads will cause capacitance changes and associated current variations.

To achieve reliable performance with MOSFET electrometers, it is necessary to provide some form of protection of the gate against the discharging of static voltages through the gate-oxide layer. Two possible methods are the neon lamp and low leakage diodes as shown in Figure 4. These protective devices do not contribute substantial leakage currents since there is practically zero volts across them under normal operating conditions.

3.2 Electrometer Circuits

A linear electrometer design with neon lamp protection is shown in Figure 5a. The A287 neon lamp has a leakage resistance greater than 10^{12} ohms, a D. C. breakdown voltage of 58 to 80 volts, and is compensated for a darkened environment. The uncompensated rise time was 125 milliseconds and the compensated rise time 50 milliseconds. Since the rise time is dependent upon the positioning of the individual components, the compensation network may vary from layout to layout and thus require determining for each layout. The design was subjected to a temperature of 80 degrees centigrade with no measurable offset voltage.

A diode protected electrometer design is shown in Figure 5b. The FJT2000 is a dual low leakage diode with a minimum breakdown voltage of 35 volts. The uncompensated rise time was found to

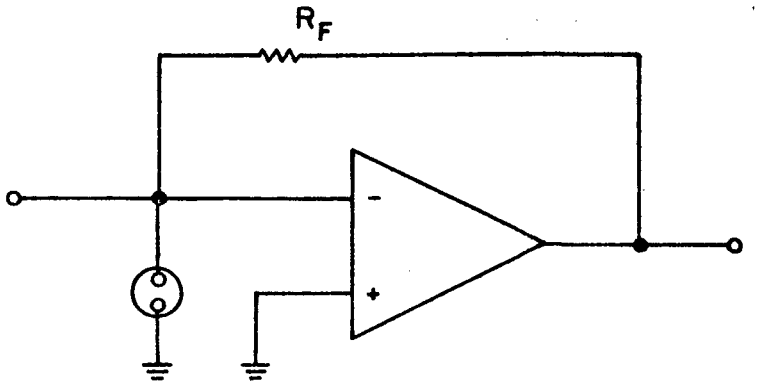

a. NEON LAMP PROTECTION

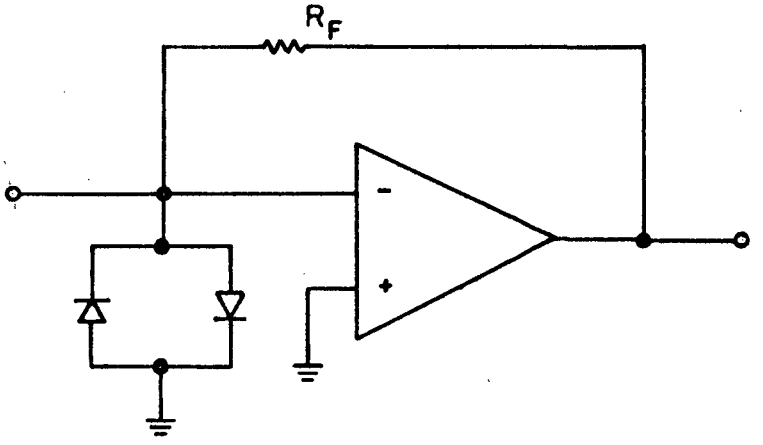

b. DIODE PROTECTION

PROTECTION SCHEMES FOR A MOSFET INPUT

FIGURE 4

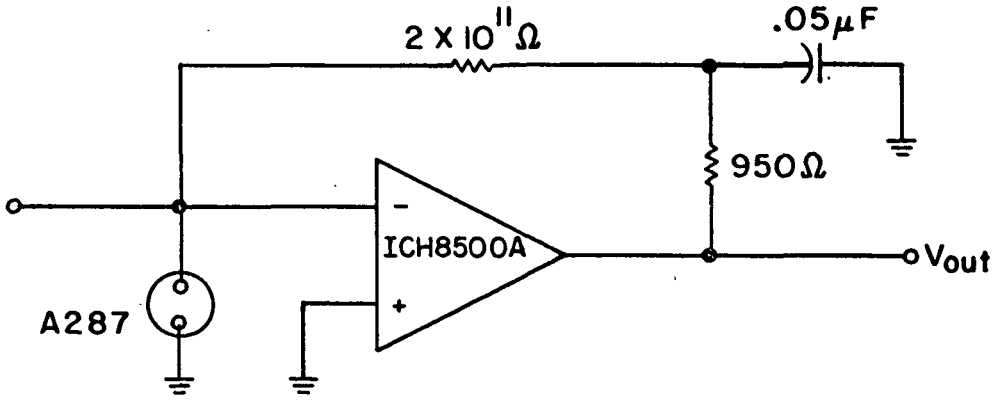

a. NEON LAMP PROTECTED ELECTROMETER

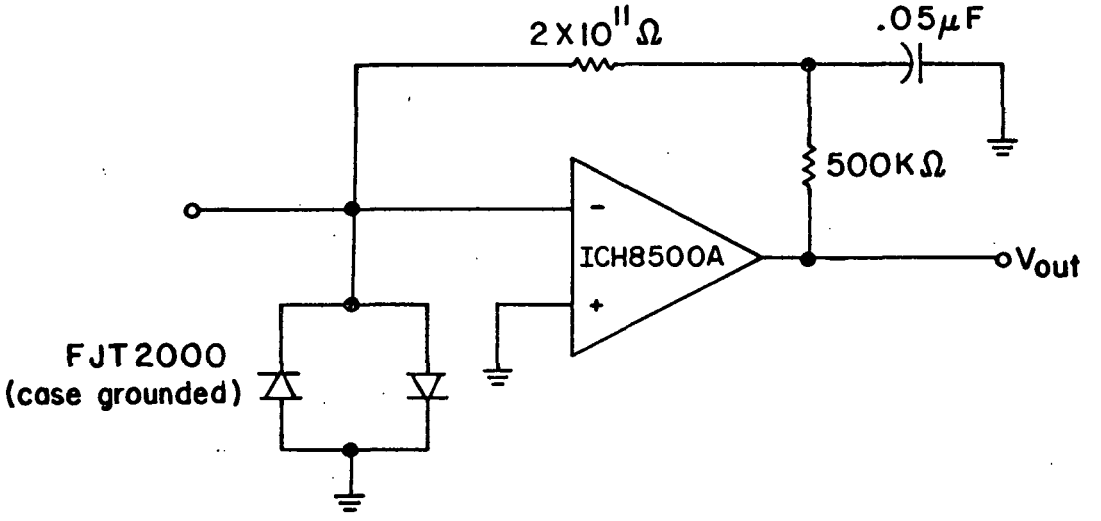

b. DIODE PROTECTED ELECTROMETER

LINEAR ELECTROMETER DESIGNS

FIGURE 5

be 130 milliseconds and the compensated rise time 50 milliseconds. Overload recovery time varied from .16 seconds to 30 seconds over a range of 1×10^{-12} to 2.5×10^{-10} coulombs of displacement charge. The design was subjected to a temperature of 80 degrees centigrade with no measurable offset voltage.

A design having a logarithmic response is shown in Figure 6. The diodes serve both as logarithmic response elements and as input protection. The desired sensitivity is achieved by appropriately selecting resistor R_S. A plot of output voltage versus input current is shown in Figure 7. The curve rises linearly to a break region beginning at .1 volts after which the rise is approximately .07 volts per decade of current. A symmetrical characteristic is obtained for negative currents. Due to the logarithmic characteristic, the frequency response is dependent upon the output level. For the linear region below .1 volts, the uncompensated rise time was 520 milliseconds, but for the linear region above .1 volts, the rise time was 10 milliseconds. Thus, compensation is required for the lower linear region and is shown in Figure 6. The rise time was decreased to 70 milliseconds. However, as a result of the dependency of rise time upon output level, overshoot occurs above a level corresponding to an input current of 1.5 pico-amperes. Thus, compensation should be provided only in very low current applications. Overload recovery time was essentially constant at 60 milliseconds over a range of 10^{-12} to 2.5×10^{-10} coulombs of displacement charge for the circuit of Figure 11. Removal of compensation components resulted in an improvement in recovery time.

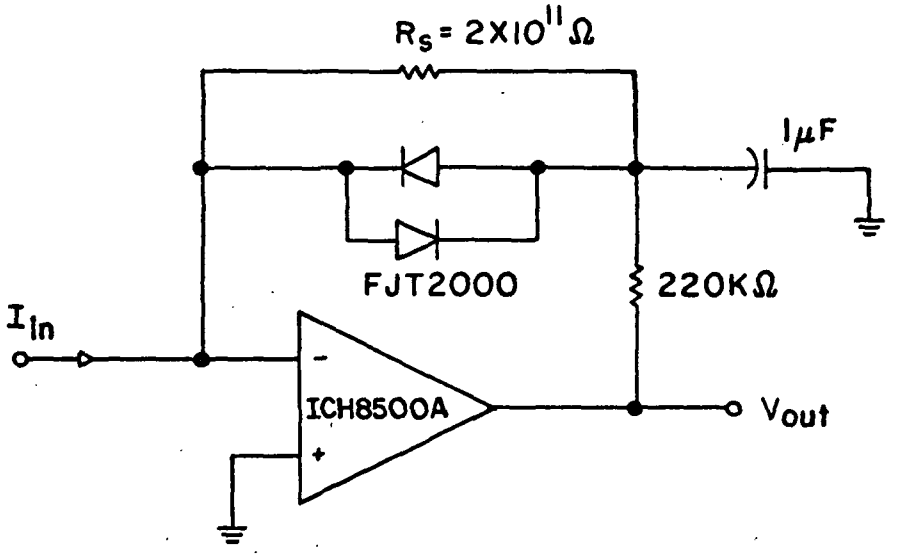

LOGARITHMIC ELECTROMETER

FIGURE 6

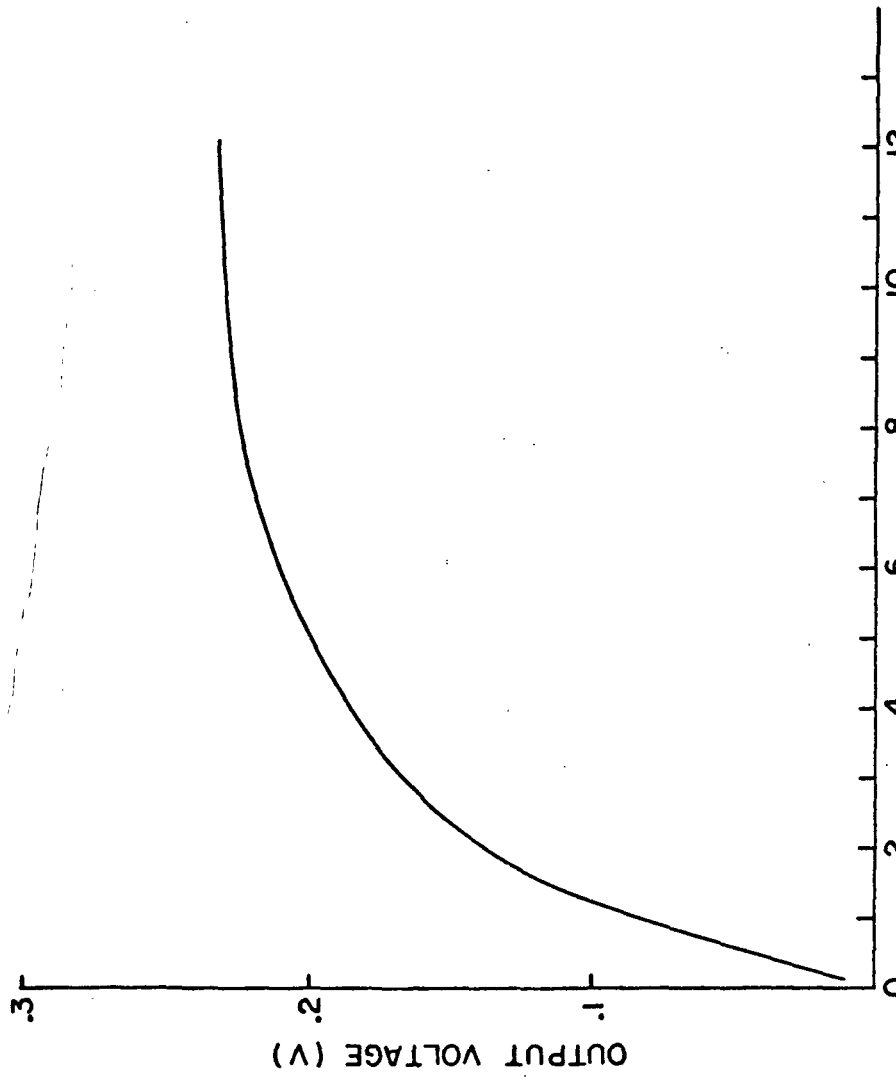

RESPONSE OF LOGARITHMIC ELECTROMETER

FIGURE 7

CHAPTER IV

SWEEP CIRCUIT DESIGN

4.1 Triangular Wave Generator

The triangular wave generator is shown in Figure 8. It consists of an integrator functioning as a ramp generator and a threshold detector functioning as the reset device. The entire operation of the circuit may be understood by considering the threshold dector to be in the positive saturation state. The detector saturation voltage is determined by zener diodes Z_1 and Z_2 and is applied to the integrator through R_3. The integrator generates a negative ramp until its output equals the trip voltage of the threshold detector. The threshold detector then changes to the negative saturation state supplying a negative voltage to the integrator. The integrator now generates a positive ramp until its output reaches the trip point of the threshold dector at which time the detector again changes state and the cycle repeats. If the positive and negative detector saturation voltages are equal, the positive and negative ramps will have equal slopes and thus a symmetrical waveform. The waveform may be offset with respect to ground if the inverting input of the threshold detector is offset with respect to ground.

Referring to Figure 9, the following design equations are appropriate. From Figure 9a, neglecting input bias current

$$I = \frac{V_{ramp} - V_{sat}}{R_1 + R_2} \quad . \tag{10}$$

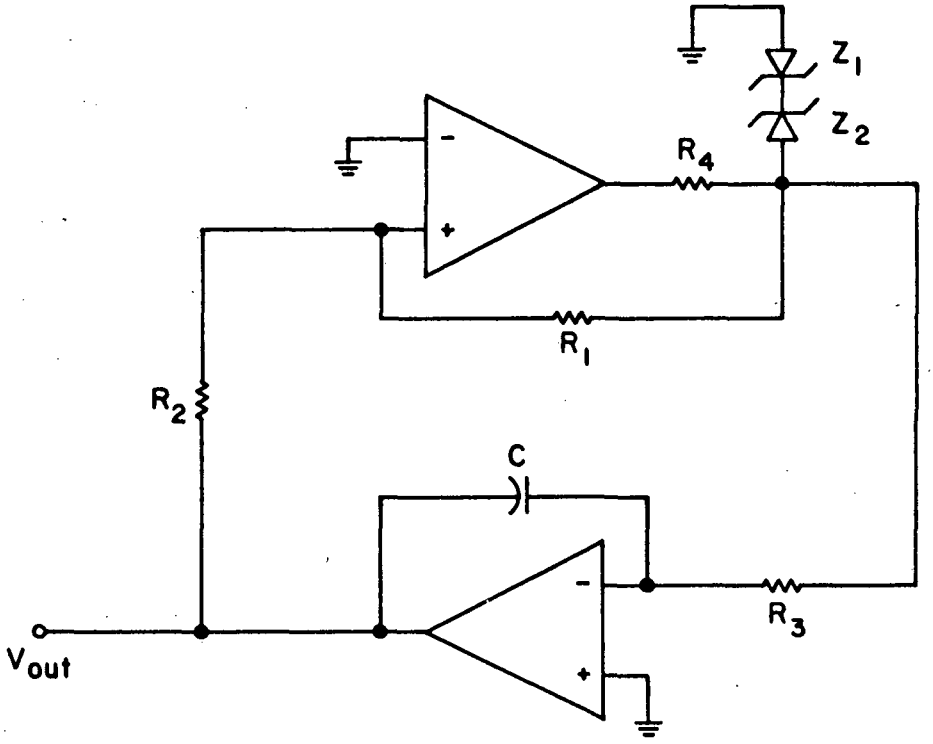

TRIANGULAR WAVE GENERATOR

FIGURE 8

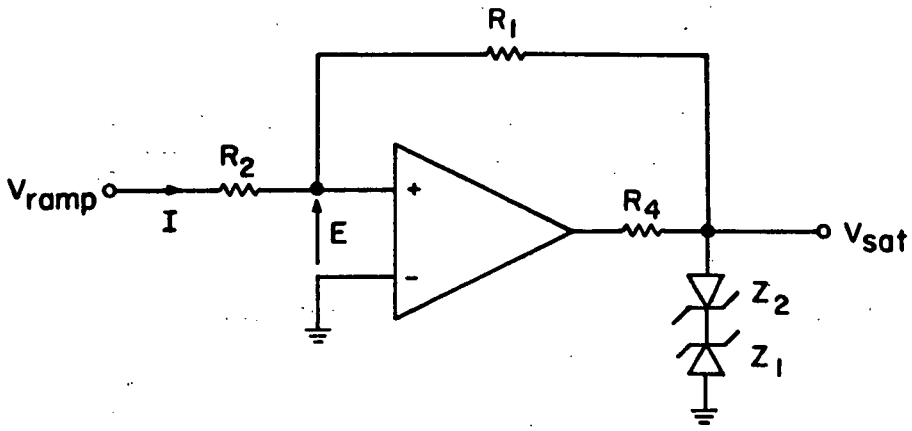

a. THRESHOLD DETECTOR

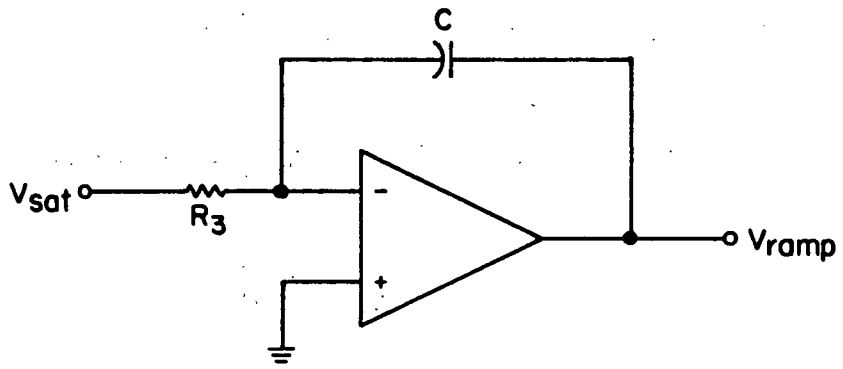

b. INTEGRATOR

CIRCUITS FOR THE DERIVATION OF DESIGN EQUATIONS

FIGURE 9

Then,

$$E = V_{ramp} - IR_2$$

$$= V_{ramp} - \frac{R_2}{R_1 + R_2} \left(V_{ramp} - V_{sat} \right)$$

$$= V_{ramp} \left(\frac{R_1}{R_1 + R_2} \right) + V_{sat} \left(\frac{R_2}{R_1 + R_2} \right) . \qquad (11)$$

Neglecting offset voltage, the threshold detector will change state when,

$$E = 0 \qquad (12)$$

or

$$V_{sat} \left(\frac{R_2}{R_1 + R_2} \right) = - V_{peak} \left(\frac{R_1}{R_1 + R_2} \right) \qquad (13)$$

where V_{peak} is the amplitude of the triangular waveform. Then,

$$V_{peak} = - \frac{R_2}{R_1} V_{sat} . \qquad (14)$$

From Figure 9b,

$$V_{ramp} = - \frac{1}{R_3 C} \int_{t_1}^{t_2} V_{sat} \, dt$$

$$= - \frac{V_{sat}}{R_3 C} (t_2 - t_1) . \qquad (15)$$

When,

$$V_{ramp} = V_{peak} \tag{16}$$

then,

$$V_{peak} = -\frac{V_{sat}}{R_3 C}\left(\frac{T}{4}\right) \tag{17}$$

where T is the period of the waveform. Note that the amplitude and frequency are independent.

4.2 Shaping Circuit

The schematic of the shaping circuit is shown in Figure 10 and its operation on the triangular waveform is described in Figure 11.

Zener diodes Z_3 and Z_4 clip the input waveform at V_3 volts and apply it to the drain of a J-FET switch. The remaining portion of the circuit then regulates the switch turning it on and off at the appropriate times.

Amplifier A_1 and associated circuitry act as an absolute value circuit. When the input voltage is negative, D_1 is forward biased and D_2 is reversed biased thus applying the input voltage to the inverting input of A_1. If R_{10} equals R_6, then the output is equal to the negative of the input. When the input is positive, D_1 is reversed biased and D_2 is forward biased thus applying the input voltage to the non-inverting input of A_1. If R_7 equals R_8 and R_{10} equals R_9, then the output equals the input.

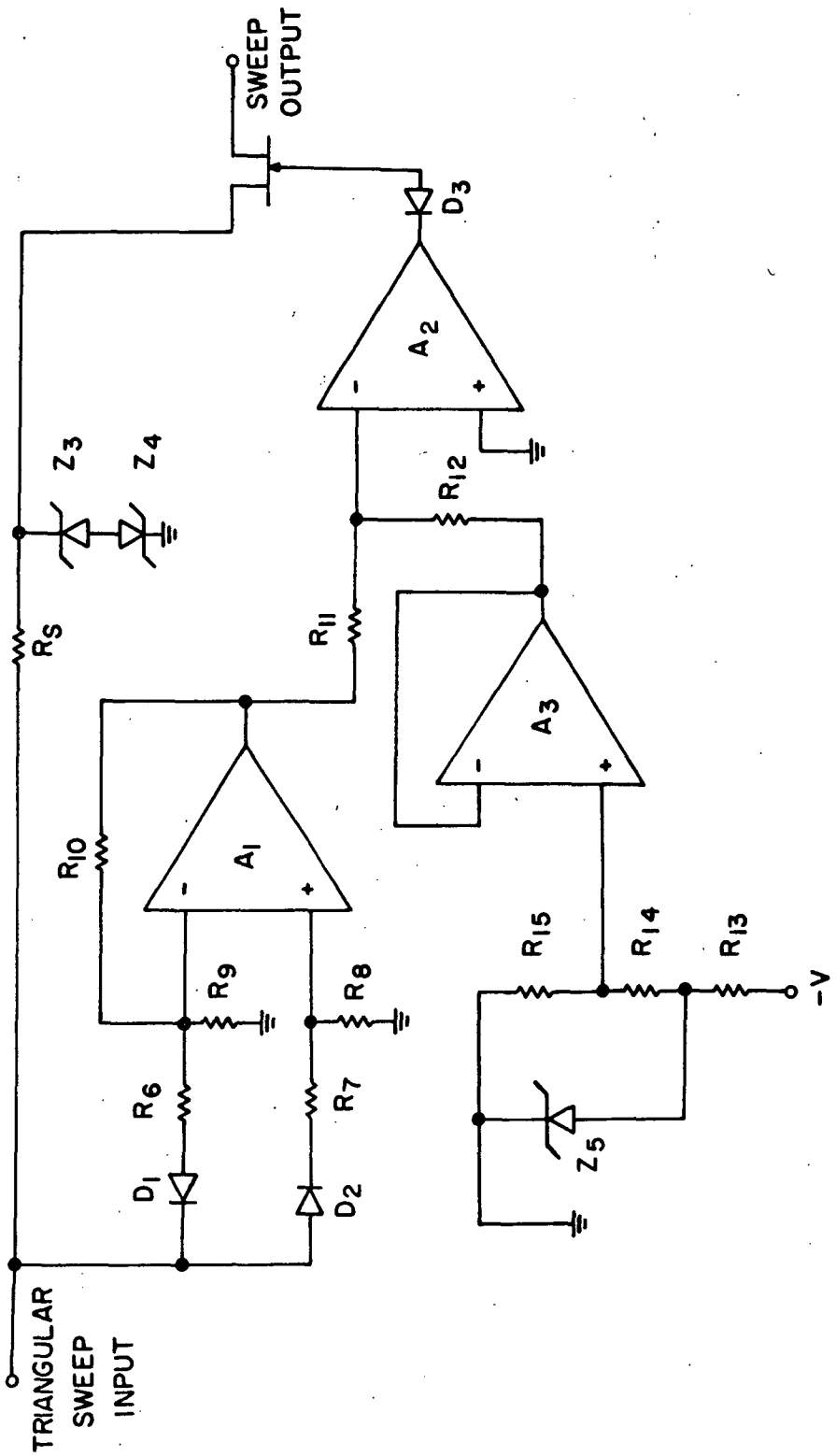

SHAPING CIRCUIT

FIGURE 10

A negative reference voltage, V_2, is generated by Z_5 and a voltage divider. The reference voltage is connected through a voltage follower, A_3, which serves as a buffer.

Amplifier A_2 is a comparator responding to the sum of the reference voltage and the rectified triangular waveform. Its saturation states are determined by the supply voltages.

The operation of the shaping circuit is now discussed with reference to Figures 10 and 11. For time zero to t_1, the sum of the reference voltage, V_2, and the triangular waveform is negative. This sum is applied to the inverting input of A_2 which saturates possitively reverse biasing D_3. The gate-source voltage of the FET is reduced to zero and the FET is turned on permitting the output to follow the triangular waveform appearing across Z_3 and Z_4. At time t_1, the triangular waveform has reached the breakdown voltage of Z_3 and is clipped. For the interval t_1 to t_2, the sum of V_2 and the triangular waveform remains negative and the output is a constant, V_3. During the interval t_2 to t_3, the sum of V_2 and the triangular waveform is positive and A_2 is saturated negatively. D_2 is forward biased and the gate-source voltage of the FET is negative turning it off and reducing the output to zero. During the interval t_3 to $\frac{T}{2}$, the sum of V_2 and the triangular waveform is again negative and the FET is turned on. The output follows the constant voltage V_3 during the interval t_3 to t_4 as the breakdown voltage of Z_3 is exceeded. For time t_4 to $\frac{T}{2}$, the triangular waveform is less than the breakdown voltage of Z_3, and the output follows the triangular waveform. During the negative portion of the cycle, the triangular waveform is rectified by A_1 permitting similar comparing and switching

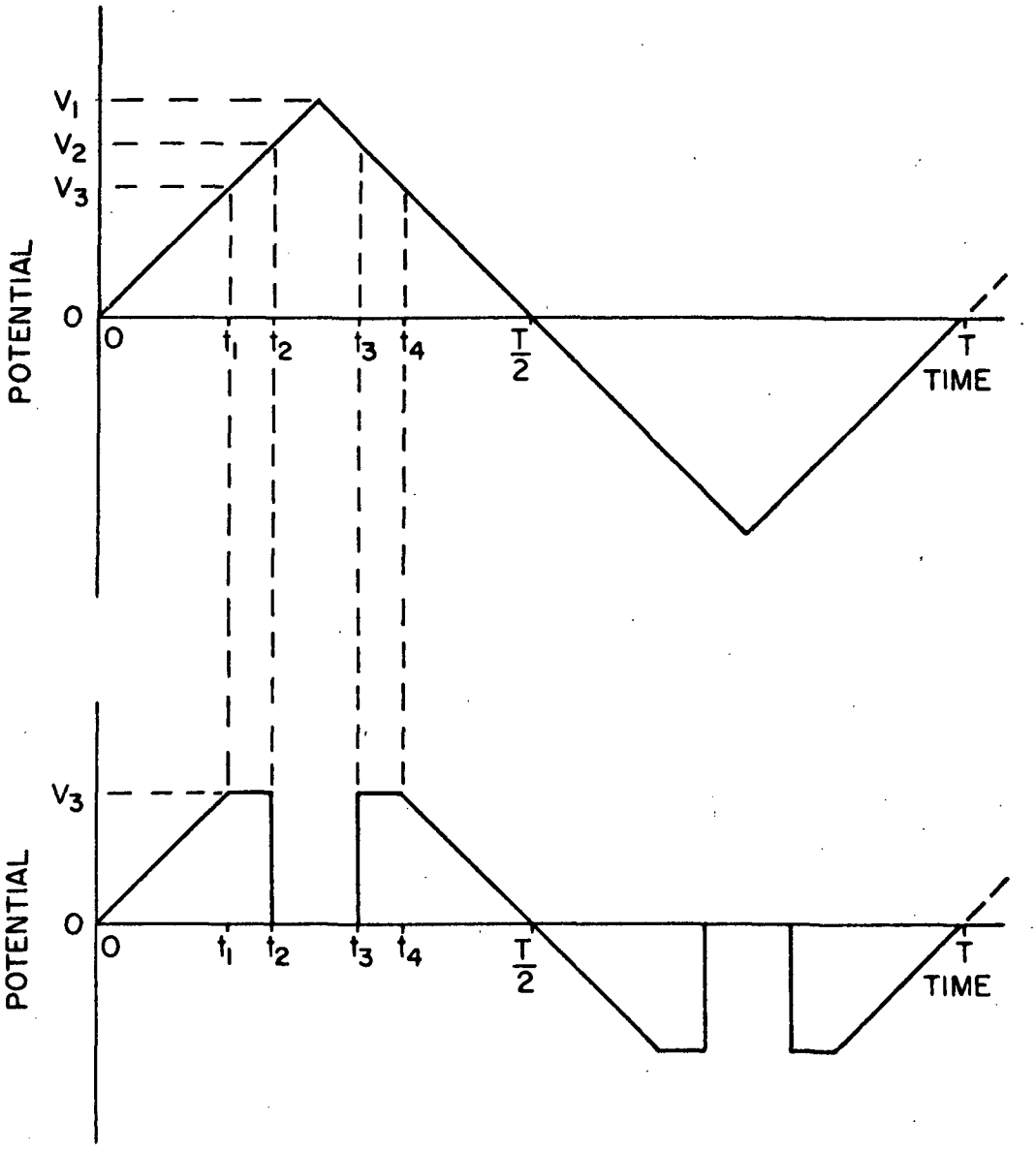

SHAPING THE TRIANGULAR WAVEFORM

FIGURE 11

operations as in the positive portion of the cycle. If Z_3 and Z_4 are identical, the negative portion of the cyle is shaped as was the positive portion.

The following design considerations are appropriate. Zener diodes Z_3 and Z_4 should require low rated current to avoid loading effects on the triangular wave generator. Resistors R_6, R_9, R_7 and R_8 must also be chosen to avoid loading effect. Resistor R_{13} should provide the rated zener current. The FET switch should be chosen to have a gate-source breakdown voltage greater than the sum of the negative saturation voltage of A_2 and V_3. Its gate-source cutoff voltage must be less than the difference between $-V_3$ and the negative saturation voltage of A_2.

A positive or negative rectified waveform may be had through slight modifications of the shaping circuit. A positive waveform is generated by the circuit in Figure 12. The triangular waveform is rectified positively by A_1 and shaped as previously discussed. The resulting output is shown in Figure 14a. A negative waveform is generated by the circuit in Figure 13. Diodes D_1 and D_2 are reversed making A_1 and its associated circuitry a negative absolute value amplifier. A positive reference voltage is required and thus Z_5 is reversed. To provide for similar switching of the FET, the reference voltage and negative waveform are coupled into the non-inverting input of A_2. The resulting output is shown in Figure 14b.

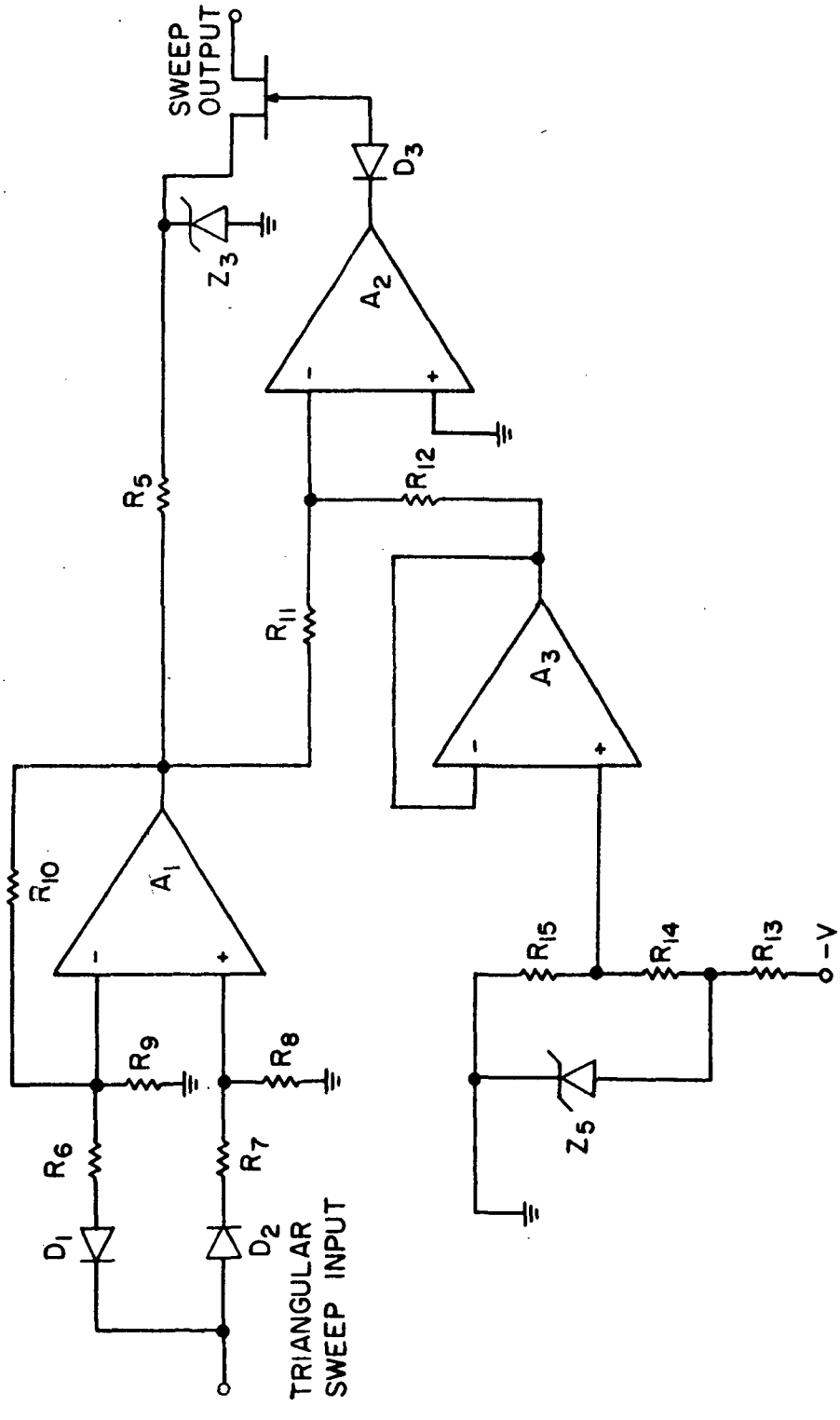

POSITIVE SHAPING CIRCUIT

FIGURE 12

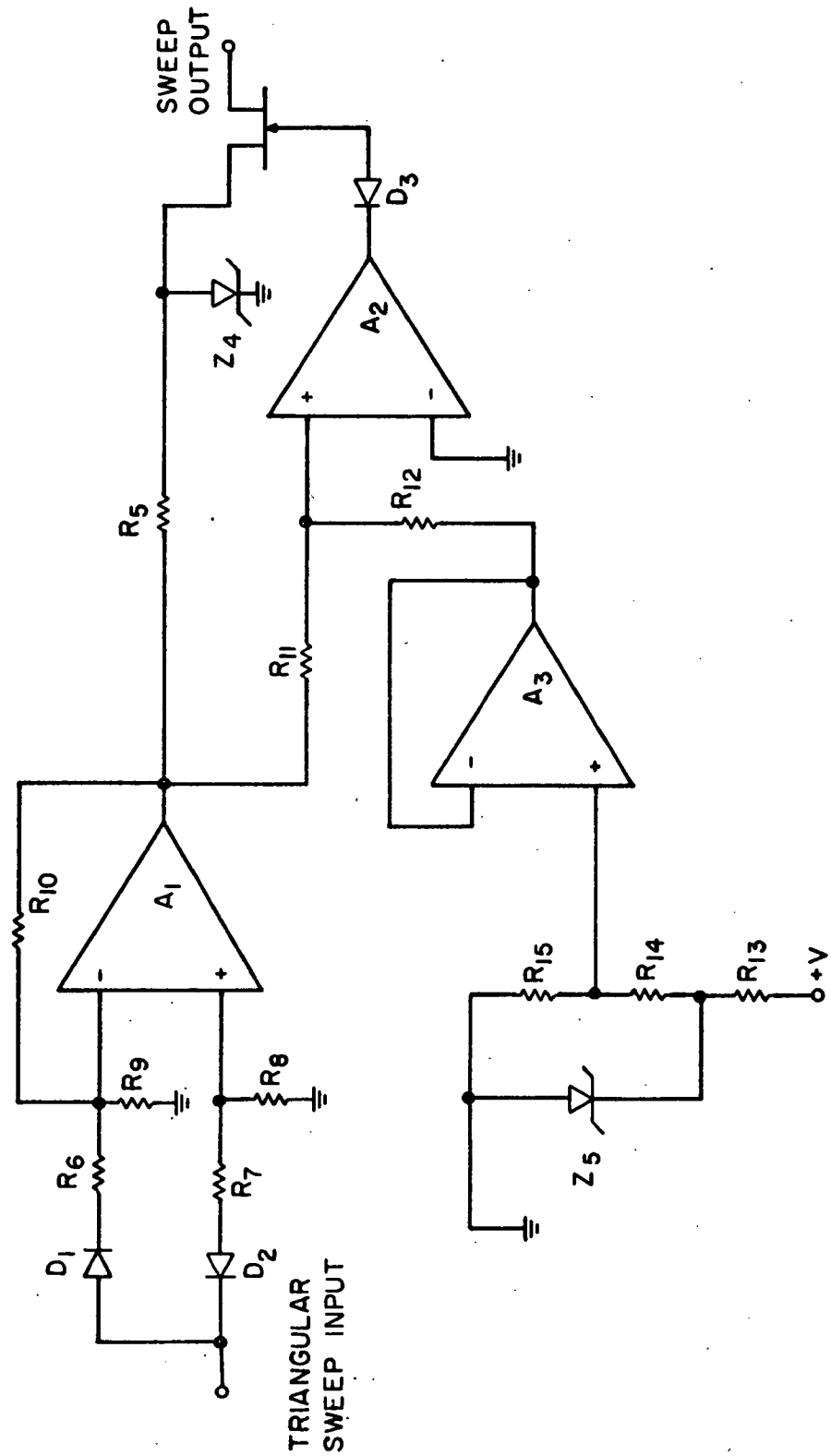

NEGATIVE SHAPING CIRCUIT

FIGURE 13

5.2 Sweep Circuit

A sweep circuit was designed to implement mobility measurements by measuring the response of a stationary probe to a step in voltage rising from zero volts. A triangular waveform is generated and subsequently shaped in the manner shown in Figure 11. The period and amplitude of the waveform may be independently adjusted as described by the design equations given in Section 4.1. The step in voltage is obtained by turning on and off an FET.

5.3 Suggestions for Future Development

To further improve the response time of the electrometer, the feedback resistor may be modified as described by Kendall (1970) through the addition of capacitive coupling between the electrometer output and the feedback resistor. This type of compensation is intended to reduce the effects of stray capacitance distributed along the length of the resistor.

To improve overload recovery time, a cancellation of displacement current is suggested. An inverted sweep waveform may be capacitively coupled into the inverting input of the electrometer. By trimming the coupling capacitor, a current equal and opposite the displacement current is injected into the summing junction.

BIBLIOGRAPHY

Hale, L. C., Private communication, 1968.

Hale, L. C., "A Probe Assembly for the Direct Measurement of Ionospheric Parameters," Scientific Report No. 223(E). Ionosphere Research Laboratory, The Pennsylvania State University, 1964.

Hale, L. C., D. P. Hoult and D. C. Baker, "A Summary of Blunt Probe Theory and Experimental Results," Space Research VII, North-Holland Publishing Company, Amsterdam, 1968.

Hale, L. C., D. P. Hoult and R. G. Willis, "Electron Density Profiles in the Ionosphere and Exosphere," North-Holland Publishing Company, Amsterdam, 1966.

Hoffman, D. J., "The Theory and Experimental Results of an Ionospheric Probe Experiment," Scientific Report No. 260, Ionosphere Research Laboratory, The Pennsylvania State University, 1966.

Hoult, D. P., Private communication, 1968.

Hoult, D. P., "D-Region Probe Theory," J. Geophys. Res., 70, 3183, 1965.

Hoult, D. P. and T. J. Kuo, "D-Region Mobility Spectrometer," J. Geophys. Res., 72, 4529, 1967.

Keller, G. E., "Use of Ionic Mobilities for Measurements in the Lower Ionosphere," J. Geophys. Res., 73, 3483, 1968.

Pontano, B. A., "An Analysis of High Ionosphere Positive Ion Ram Probes," Scientific Report No. 291, Ionosphere Research Laboratory, The Pennsylvania State University, 1967.

Praglin, J. and W. A. Nichols, "High-Speed Electrometers for Rocket and Satellite Experiments," Proc. IRE, 48, 771, 1960.

Sonin, A. A., "Theory of Ion Collection by Supersonic Atmospheric Sounding Rocket," J. Geophys. Res., 72, 4547, 1967.

Willis, R. G., "A Subsonic Probe for the Measurement of D-Region Charged Particle Densities," Scientific Report No. 245, Ionosphere Research Laboratory, The Pennsylvania State University, 1965.

GENERAL REFERENCES

Archambault, Jan, "The Ubiquitous Electrometer," Industrial Research, 36, 1971.

Homiller, W. T., "Small Current Measurements with Insulated Gate Field Effect Transistors," Scientific Report No. 284(E), Ionosphere Research Laboratory, The Pennsylvania State University, 1966.

Phalan, J., "Ultra Low Bias Current Operational Amplifier," Application Bulletin H001, Intersil, Inc., 1970.

Seymour, Ralph and Leonard Brown, "Designing with Diff-Amp and Op-Amp IC's," EEE, 17, 59, 1969.

"ICH8500/ICH8500A Ultra Low Bias Current Operational Amplifier," Data Sheet, Intersil, Inc., 1970.

"Models 310, 311 Ultra Low Bias Current Varactor Bridge Operational Amplifiers," Data Sheet, Analog Devices, Inc., 1969.

"FET-Input Op Amp Offers Low Bias Current," EEE, 18, 22, 1970.